


RESEARCH PAPER



ESRRA (estrogen related receptor, alpha) induces ribosomal protein RPLP1-mediated adaptive hepatic translation during prolonged starvation

Madhulika Tripathi^{a*}, Karine Gauthier^{b*}, Reddemma Sandireddy^a, Jin Zhou^a, Priyanka Gupta^a, Suganya Sakthivel^a, Nah Jiemin^c, Kabilesh Arul^a, Keziah Tikno^a, Sung-Hee Park^d, Yajun Wu^e, Lijin Wang^f, Boon-Huat Bay^e, Lena Ho^c, Vincent Giguere^g, Sujoy Ghosh^{f,h}, Donald P. McDonnell^d, Paul M. Yen^{a,i}, and Brijesh K. Singh 

^aLaboratory of Hormonal Regulation, Cardiovascular and Metabolic Disorders Program, Duke-National University of Singapore (NUS) Medical School, Singapore, Singapore; ^bDépartement de Biologie, Institut de Génomique Fonctionnelle de Lyon, Université de Lyon, Université Lyon 1, CNRS, Ecole Normale Supérieure de Lyon, Lyon, Cedex, France; ^cCardiovascular and Metabolic Disorders Program, Duke-National University of Singapore (NUS) Medical School, Singapore, Singapore; ^dDepartment of Pharmacology and Cancer Biology, Duke University School of Medicine, Durham, NC, USA; ^eDepartment of Anatomy, Yong Loo Lin School of Medicine, NUS, Singapore, Singapore; ^fCentre for Computational Biology, Cardiovascular and Metabolic Disorders Program, Duke-National University of Singapore (NUS) Medical School, Singapore, Singapore; ^gGoodman Cancer Research Centre, McGill University, Montreal, Québec, Canada; ^hPennington Biomedical Research Center, Laboratory of Bioinformatics and Computational Biology, Baton Rouge, LA, USA; ⁱDuke Molecular Physiology Institute and Department of Medicine, Duke University School of Medicine, Durham, NC, USA

ABSTRACT

Protein translation is an energy-intensive ribosome-driven process that is reduced during nutrient scarcity to conserve cellular resources. During prolonged starvation, cells selectively translate specific proteins to enhance their survival (adaptive translation); however, this process is poorly understood. Accordingly, we analyzed protein translation and mRNA transcription by multiple methods *in vitro* and *in vivo* to investigate adaptive hepatic translation during starvation. While acute starvation suppressed protein translation in general, proteomic analysis showed that prolonged starvation selectively induced translation of lysosome and autolysosome proteins. Significantly, the expression of the orphan nuclear receptor, ESRRA (estrogen related receptor, alpha) increased during prolonged starvation and served as a master regulator of this adaptive translation by transcriptionally stimulating *Rplp1* (ribosomal protein lateral stalk subunit P1) gene expression. Overexpression or siRNA knockdown of *Esrra* *in vitro* or *in vivo* led to parallel changes in *Rplp1* gene expression, lysosome and macroautophagy/autophagy protein translation, and autophagy activity. Remarkably, we have found that ESRRA had dual functions by not only regulating transcription but also controlling adaptive translation via the ESRRA-RPLP1-lysosome-autophagy pathway during prolonged starvation.

ARTICLE HISTORY

Received 22 January 2024
Revised 31 January 2025
Accepted 6 February 2025

KEYWORDS



60S acidic ribosomal protein P1 (RPLP1); autophagy; estrogen related receptor alpha (ESRRA/ERRα); lysosome; starvation; translation

Introduction


Cells undergo adaptations to conserve energy during periods of nutrient scarcity or starvation. During acute starvation, there is suppression of protein translation, a vital cellular process by which ribosomes translate information from messenger RNA (mRNA) to synthesize proteins. However, during prolonged starvation, selective protein translation occurs in order to ensure cell survival (adaptive translation) [1–3]. Adaptive translation not only conserves vital resources but also shifts the utilization of cellular machinery and resources toward processes that help the cell to manage stress and enhance viability. It is tightly controlled and includes the selective protein translation of lysosome and autolysosome proteins involved in autophagy and other cellular catabolic processes [4,5]. In the liver, activation of lysosome-autophagy is crucial for maintaining the amino acid pool vital for translating proteins that oversee life-sustaining processes during

starvation such as mitochondrial activity and β -oxidation of fatty acids [6–11].

Although nuclear receptors are known to regulate transcription, their influence(s) on protein translation is not known. The orphan nuclear receptor ESRRA/ERRα, (estrogen related receptor, alpha) plays a crucial role in various metabolic processes [10]. Unlike classical estrogen receptors, ESRRA does not bind to endogenous estrogens but instead regulates gene expression by binding to estrogen-related response elements (ERREs) in target gene promoters [12]. ESRRA is primarily expressed in tissues with high energy demands, such as the heart, skeletal muscle, and liver, where it functions as a key regulator of mitochondrial biogenesis, oxidative metabolism, and energy homeostasis [10,13]. ESRRA exerts its regulatory effects by forming heterodimers with PPARGC1A/PGC-1α (peroxisome proliferative activated receptor, gamma, coactivator 1 alpha) [10]. This partnership enhances the transcriptional activity of ESRRA, leading to the

CONTACT Brijesh K. Singh  singhbrijeshk@duke-nus.edu.sg  Cardiovascular and Metabolic Disorders Program, Duke-NUS Medical School, 8 College Road, Singapore 169857, Singapore

*Authors share equal contribution.

 Supplemental data for this article can be accessed online at <https://doi.org/10.1080/15548627.2025.2465183>

© 2025 The Author(s). Published by Informa UK Limited, trading as Taylor & Francis Group.

This is an Open Access article distributed under the terms of the Creative Commons Attribution-NonCommercial-NoDerivatives License (<http://creativecommons.org/licenses/by-nc-nd/4.0/>), which permits non-commercial re-use, distribution, and reproduction in any medium, provided the original work is properly cited, and is not altered, transformed, or built upon in any way. The terms on which this article has been published allow the posting of the Accepted Manuscript in a repository by the author(s) or with their consent.

upregulation of genes involved in mitochondrial function, fatty acid oxidation, and oxidative phosphorylation. The ESRRA-PPARGC1A axis is particularly important for maintaining genes' transcription regulating energy balance during metabolic stress, such as fasting or exercise [14,15]. ESRRA is a central player in this adaptive response during periods of nutrient deprivation. ESRRA was shown to be upregulated during fasting to stimulate the expression of genes involved in mitochondrial respiration and fatty acid oxidation [12]. ESRRA also was shown to promote gluconeogenesis for maintaining blood glucose levels during fasting [16]. Furthermore, ESRRA has been shown to regulate the expression of genes involved in autophagy and mitophagy to release free fatty acids for sustained β -oxidation [13,17]. This process is critical for sustaining energy production during prolonged fasting when carbohydrate stores are depleted. Through these mechanisms, ESRRA helps to optimize energy utilization and maintain metabolic homeostasis during nutrient scarcity.

While ESRRA's role in transcriptional regulation of metabolic genes is well-established, its involvement in protein translation regulation was not previously known. Our study has uncovered a novel function of ESRRA in regulating adaptive protein translation during starvation. We demonstrated that ESRRA induces the expression of the ribosomal protein RPLP1, which in turn enhances the translation of lysosomal and autophagy-related proteins. This ESRRA-RPLP1 pathway is crucial for maintaining autophagy. The discovery that ESRRA regulates protein translation adds a new layer of complexity to our understanding of its role in metabolism. It highlights the dual function of ESRRA in both transcriptional and translational control, underscoring its importance in coordinating cellular responses to metabolic stress. This regulatory mechanism ensures that cells can adapt to prolonged fasting by selectively translating proteins necessary for autophagy and lysosomal function, thereby maintaining cellular homeostasis and survival.

Results

Selective protein translation activity was temporally regulated

Puromycin is an aminonucleoside that mimics the 3' end of aminoacylated tRNAs and is incorporated into the C terminus of nascent protein chains during the ribosome-mediated protein synthesis [18]. To understand protein translation activity during acute and prolonged starvation, we performed puromycin-labeling of nascent proteins to evaluate their ribosome-mediated protein translation [18–21]. Accordingly, mice were starved for 8, 24 or 48 h, followed by puromycin-labeling (*i.p.* 20 mg/kg for 30 min just before the euthanization of mice) of newly translated proteins. The mice exhibited a time-dependent decrease in puromycin-labeled proteins at 8 h and 24 h in the liver followed by partial translational recovery at 48 h (Figure 1A). Similarly, primary human hepatocytes and mouse hepatic cells (AML12) cultured in serum-free media (serum starvation) for 0, 6, 24, 48, and 72 h, followed by puromycin labeling for a brief period (10 μ g/ml for 15 min before the protein isolation), showed decreased puromycin-

labeling from 6 h to 48 h serum starvation and partial recovery at 72 h in both hepatic cell lines (Figure 1B,C). We next performed polysome profiling to confirm the puromycin-labeled protein findings (Figure 1D). We observed decreased polysome peaks at 48 h serum starvation compared to 0 h suggesting reduced polysome-occupied mRNAs and translation activity at that time point. Interestingly, polysome peaks increased at 72-h serum starvation compared to 48 h, indicating there was a partial recovery in translation activity during prolonged starvation.

To analyze translated proteins at 48- and 72-h serum starvation, we performed an unbiased label-free quantitative/LFQ proteomic analysis in AML12 cells that underwent serum starvation for 0, 48 and 72 h (Figure S1A). Surprisingly, despite the decrease in overall translation rate at 48-h serum starvation, approximately 10% of detectable proteins in the total proteome (445/4082 proteins) increased expression (>50% higher expression than 0 h baseline) at 48 h, whereas 20% of detectable proteins in the total proteome (848/4066 proteins) increased at 72 h of serum starvation (Figure 1E), suggesting there was adaptive protein synthesis during prolonged starvation. We next analyzed all upregulated proteins at both time points to identify major induced pathways using the Gene Ontology Cellular Components (GO CC) 2018 databases and Kyoto Encyclopedia of Genes and Genomes (KEGG) 2019 (Figure 1F, Figure S1B). Interestingly, 55% of the total up-regulated proteins were induced exclusively at 72-h serum starvation and enriched for pathways regulating ribosomes, polysomes, RNA transport, ribosome biogenesis, autolysosomes, as well as lysosomes in the KEGG analysis (Figure 1G, Figure S1B, Tables S1–3). Fourteen percent of the total upregulated proteins were exclusively induced at 48 h of starvation but did not correlate with any pathway (Table S1, S4 and S5). Similar findings for pathways uniquely upregulated at 48 and 72 h of starvation also were observed in GO CC analyses (Tables S6–8). Interestingly, 31% of the upregulated proteins were commonly induced at both 48- and 72-h serum starvation (Figure 1G). KEGG analyses of the commonly induced proteins revealed pathways related to lysosomes, fatty acid degradation, and mitochondrial oxidative phosphorylation (OXPHOS) (Figure 1F,G, Figure S1C, Table S1). Likewise, GO CC analysis confirmed that mitochondria and lysosomes were among the most significantly upregulated cellular components induced at both 48 and 72 h of starvation (Figure S1C; Tables S6–8).

Selective induction of ribosome, lysosome and autolysosome proteins in hepatic cells during prolonged starvation

When we analyzed the expression of individual proteins, we found that many of the proteins belonging to the ribosome pathway were downregulated after 48-h serum starvation compared to baseline but rose to higher levels than baseline after 72 h (Figure S1B). Surprisingly, RPLP1, a ribosomal large subunit protein induced during embryonic development of the nervous system [22], was one of the most upregulated ribosomal proteins in adaptive translation occurring at 72-h serum starvation. Interestingly, the expression of many of the

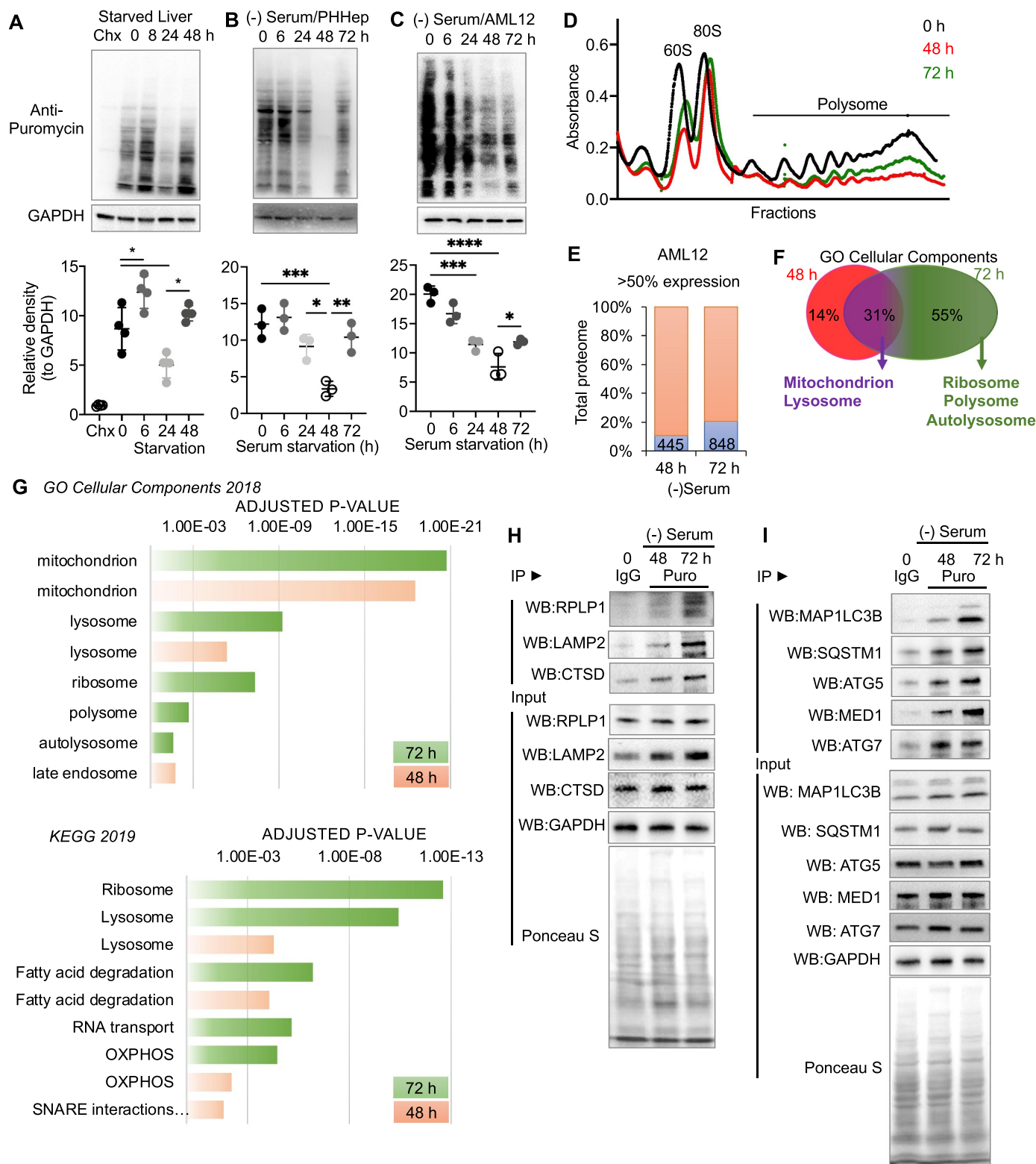


Figure 1. Hepatic protein translation was temporally regulated in starvation. (A-C) Representative western blots of puromycin-labeled proteins in starved livers ($n = 4$ per group), serum-starved primary human hepatocytes (PHHep; $n = 3$ per group), and AML12 cells ($n = 3$ per group). Cycloheximide (Chx, 10 mg/kg body weight for 60 min) for translation inhibition and puromycin (Puro, 20 mg/kg body weight for 30 min) for protein labeling of nascent proteins were used just before euthanization for indicated time points. Dot plots below the western blots represent relative density is normalized to GAPDH. (D) Graph represents polysome profile in AML12 cells under 0, 48, and 72 h serum starvation, confirming puromycin-labeling results for translation activity. (E) Graph represents the percent of total number of upregulated (>50% expression compared to 0 h) proteins (absolute number in the bars) from a label-free quantification by mass spectrometry. (F) Venn analysis for common (purple) and exclusive (red for 48 h, and green for 72 h) pathways. (G) Graphs representing significant pathways analyzed using Gene Ontology (GO) Cellular Components and KEGG 2018 database on EnrichR platform (the Ma'ayan Lab, NY, USA). (H and I) Immunoprecipitation of puromycin-labeled proteins to analyze newly synthesized proteins and their detection using western blotting. Ponceau S staining of the membranes showing protein content in each lane. Figures are showing a representative western blot $n = 3$. Levels of significance: * $p < .05$; ** $p < .01$; *** $p < .001$; **** $p < .0001$.

lysosomal proteins also were modestly upregulated at 48-h compared to the baseline (Figure S1B) with the notable exceptions of MAN2B1, GLA, and GM2A which were downregulated. Significantly, the expression of almost all the lysosomal proteins, including CTSD and LAMP2 as well as MAN2B1, GLA, and GM2A, were higher at 72-h than at 48-h (Figure S1B). Additionally, expression of proteins involved in fatty acid oxidation (*e.g.*, ACOX3, ACAA2, and HADHA) and OXPHOS (*e.g.*, NDUFA9, NDUFB9, and SDHA) modestly increased at 48-h and further increased at 72-h serum starvation (Figures S1B), consistent with the notion that sustained mitochondrial activity was required for fatty acid β -oxidation for cell survival during starvation. To validate the proteomics data, we performed puromycin immunoprecipitation of puromycin-labeled proteins at 0-, 48- and 72-h and found that RPLP1 was highly enriched at 72-h whereas lysosomal proteins, LAMP2 and CTSD were slightly enriched at 48-h, and further enriched at 72-h (Figure 1H). Moreover, qPCR analysis of polysome fractions from AML12 cells revealed that *Rplp1*, *Lamp1*, and *Ctsd* mRNA were enriched in polysome-occupied fractions (*i.e.*, mRNAs encoding high abundance proteins) at 72-h serum starvation compared to 0 or 48 h (Figures S1C and D).

Starvation-induced autophagy is dependent upon lysosome-mediated catabolism [23,24]. Accordingly, we examined puromycin-labeling of several autophagy proteins: MAP1LC3B, SQSTM1, ATG5, and ATG7 as well as MED1, an autophagy regulatory co-activator protein [25], and found they had similar temporal patterns of puromycin-labeling as lysosome proteins (Figure 1I) except for ATG7 which had increased puromycin-labeling at 48-h but no further change at 72-h. Proteomic analysis also revealed that MAP1LC3B, SQSTM1, ATG5, and MED1 protein expression increased at 72-h compared to 48-h, whereas ATG7 protein expression remained the same at 72-h (Figure S1B). Thus, activation of ribosome-mediated induction of protein translation helped maintain both lysosome and autophagy protein expression in hepatic cells at 72-h serum starvation.

ESRRA regulation of ribosome-catalyzed translation of lysosome proteins in hepatic cells during prolonged starvation

We next performed a transcription factor analysis by Targeting Protein-Protein Interaction (TF PPIs) of upregulated proteins and identified PPARGC1A and ESRRA as the transcription factors most likely involved in the increases in protein translation at 72 h of serum starvation (Figure 2A). PPARGC1A is a heterodimer partner of ESRRA [13], so it is noteworthy that previous studies in *ppargc1a* knockout (KO) mice displayed decreased LAMP2 and CTSD expression in vascular smooth muscle cells [26]. We and others also previously demonstrated ESRRA transcriptionally regulated autophagy and mitophagy and stimulated its own transcription [13,27–29]. However, its role in the regulation of translation was not known. Moreover, the ERR subfamily of nuclear receptors comprised of ESRRA, ESRRB, and ESRRG isoforms [13,17]. However, we confirmed that ESRRA is the prominent ERR isoform in human and mice liver (Figures S2A and B).

To understand the role of ESRRA in the transcriptional regulation of *Esrra* and *Rplp1* genes during starvation, we analyzed hepatic ESRRA ChIP-seq data and found that ESRRA bound to its own promoter (Figure 2B), suggesting its transcription was involved in a positive-feedback loop [13,30]. ESRRA also bound specifically to the *Rplp1* gene promoter (Figure 2A), the most upregulated ribosomal protein during serum starvation in AML12 cells (Figures S1B). Of note, ESRRA was not observed to bind to any of the other ribosomal gene promoters ranked among the top ten. Thus, to confirm if ESRRA regulated *Rplp1* transcription and RPLP1-mediated translation during serum starvation, we performed RT-qPCR analysis for *Esrra* and *Rplp1* gene expression (Figure 2C). Consistent with the hepatic ESRRA ChIP-seq data, serum starvation induced *Esrra* and *Rplp1* gene expression in a time-dependent manner from 48-h to 72-h serum starvation. Interestingly, *Esrra* siRNA knockdown (KD) in AML12 cells completely blocked the increase in *Rplp1* gene expression at 72-h serum starvation and suggested ESRRA regulated *Rplp1* gene expression during prolonged serum starvation. Moreover, decreased polysome peaks in *Esrra* siRNA KD cells showed that *Esrra* KD completely inhibited protein translation at 72-h serum starvation (Figure 2D). Further, *Esrra* KD completely inhibited the enrichment of *Esrra*, *Rplp1*, *Lamp2*, and *Sqstm1* mRNA in polysome-occupied fractions (Figure S3A); thus, supporting the notion that their active translation was ESRRA-RPLP1-dependent. Additionally, *Esrra* or *Rplp1* KD in AML12 cells inhibited overall puromycin-labeled proteins and puromycin labeling of LAMP2, CTSD, and MAP1LC3B-II proteins whereas puromycin labeling of SQSTM1 protein increased. These data suggested that reduced expression of either ESRRA or RPLP1 proteins decreased protein translation, expression of lysosomal proteins, and autophagy (Figure 2E–G). In contrast, overexpression of either ESRRA or RPLP1 in AML12 cells significantly increased puromycin-labeling of LAMP2, CTSD, MAP1LC3B-II, and SQSTM1 proteins (Figure 2H–J), and suggested that activation of either ESRRA or RPLP1 stimulated their translation.

Because autophagy is a highly adaptive and dynamic process where lysosomes play key roles in degradation and nutrient recovery during starvation [31,32], we examined a more detailed time course of ESRRA, RPLP1, lysosome protein (LAMP2 and CTSD) and autophagy protein (MAP1LC3B-II and SQSTM1) expression in AML 12 cells at baseline, 6, 24, 48, and 72 h of serum starvation (Figure 3B). ESRRA expression increased during both acute and prolonged starvation whereas MAP1LC3B-II protein expression was high at 24 h, decreased at 48 h, and then increased again at 72 h whereas SQSTM1 expression rose slightly at 48 h and returned back to baseline at 72 h, consistent with a decline and resumption of autophagy. These changes in MAP1LC3B-II protein expression were mirrored by expression of RPLP1, LAMP2, and CTSD proteins (Figures S3B–D) and further supported the role of ESRRA and RPLP1 in regulating the recovery of both autophagy and lysosome proteins during prolonged starvation.

Next, we confirmed lysosomal activity, autophagy flux, and mitochondrial activity in AML12 cells transfected with or

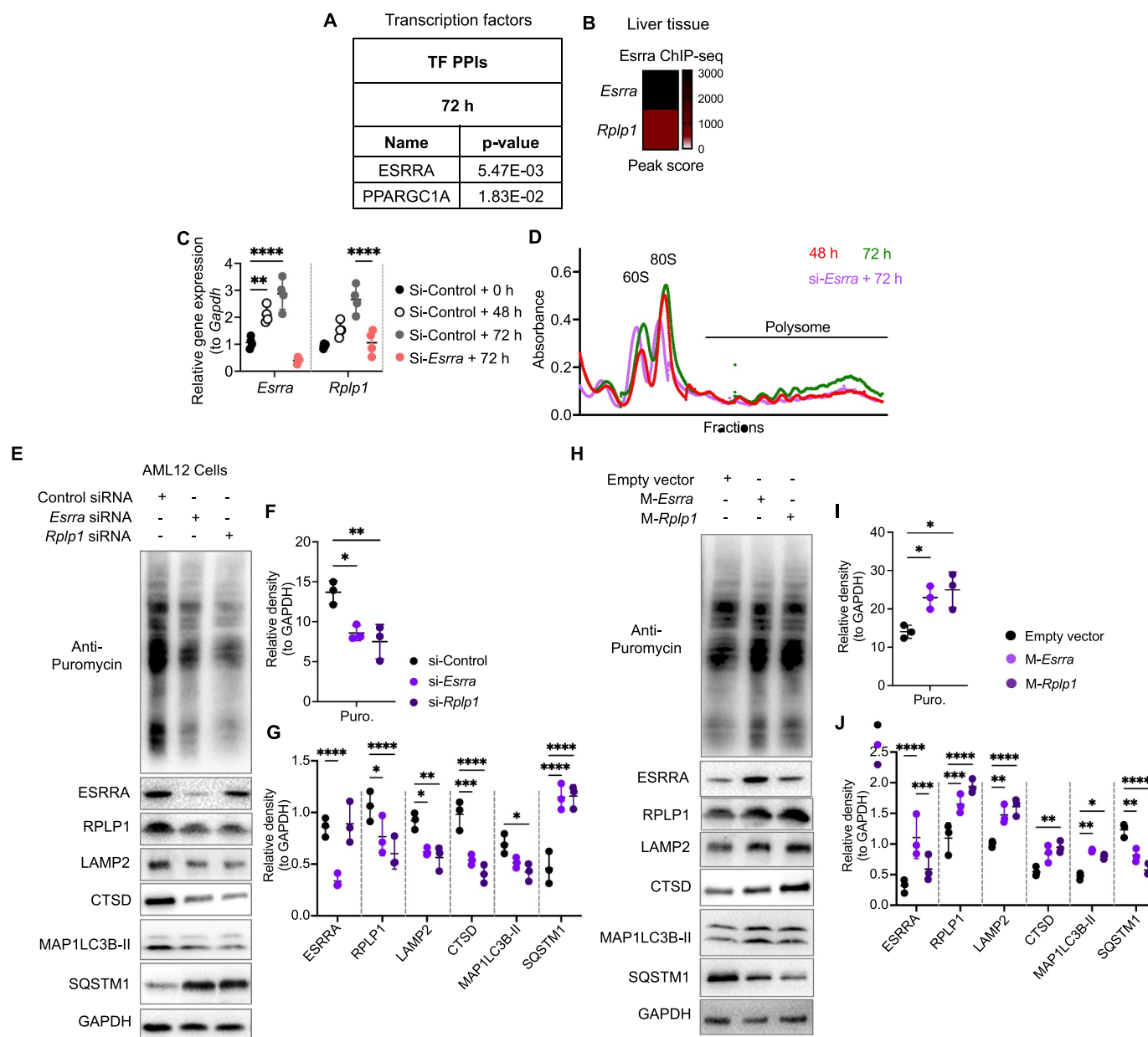


Figure 2. ESRRA regulated ribosomal RPLP1 transcription, protein translation and the expression of lysosome and autophagy proteins in serum starvation. (A) Transcription factor analysis for > 50% expressed proteins in 72 h serum-starved AML12 cells compared to 48 h using Targeting Protein-Protein Interactions (PPIs) on EnrichR platform (the Ma'ayan Lab, NY, USA). (B) Heat map shows peak score of ESRRA ChIP-seq analysis in liver tissues published previously [13]. (C) RT-qPCR analysis of control and serum-starved AML12 cells (for the indicated time points) with or without si-Esrra. Relative gene expression is normalized to *Gapdh*. (D) Graph represents polysome profiling in AML12 cells under 48 h, 72 h of serum starvation and 72-h serum starvation with si-Esrra KD conditions. (E) Representative western blots of AML12 cells treated with control, si-Esrra or si-Rplp1 for 72 h. (F and G) Plots represent relative density of western blots normalized to GAPDH. (H) Representative western blots of AML12 cells treated with empty plasmid, mouse *Esrra* or *Rplp1* expressing plasmid for 72 h. (I and J) Plots represent relative density of western blots normalized to GAPDH. Levels of significance: * $p < .05$; ** $p < .01$; *** $p < .001$; **** $p < .0001$.

without *Esrra* siRNA during serum starvation as found earlier (Figure 1F,G). We used acridine orange (AO) staining to analyze lysosomal activity [33] and found, consistent with the pathway analysis data (Figure 1G), AO staining increased during serum starvation in control AML12 cells. In contrast, it decreased in *Esrra* siRNA KD cells (Figure 3A,B). These data confirmed that lysosomal activity increased during serum starvation and decreased when *Esrra* was knocked down. To demonstrate that ESRRA-mediated autophagic flux increased during starvation, we transiently expressed RFP-eGFP-*Map1lc3* plasmid in AML12 cells transfected with control

and *Esrra* siRNAs, and undergoing serum starvation (Figure 3C-E). We observed increased red puncta formation in control siRNA treated cells (Figure 3D) indicating that there was an increase in autophagy flux since GFP fluorescence was quenched in active lysosomes [13,34]. In contrast, there were increased yellow puncta in *Esrra* siRNA-treated cells in serum-containing media and even more in serum-free media (Figure 3E). The increased yellow puncta arose from increased fluorescence of both GFP and RFP due to inhibition of autophagy flux. We further confirmed these findings by performing transmission electron microscopy (TEM) (Figures

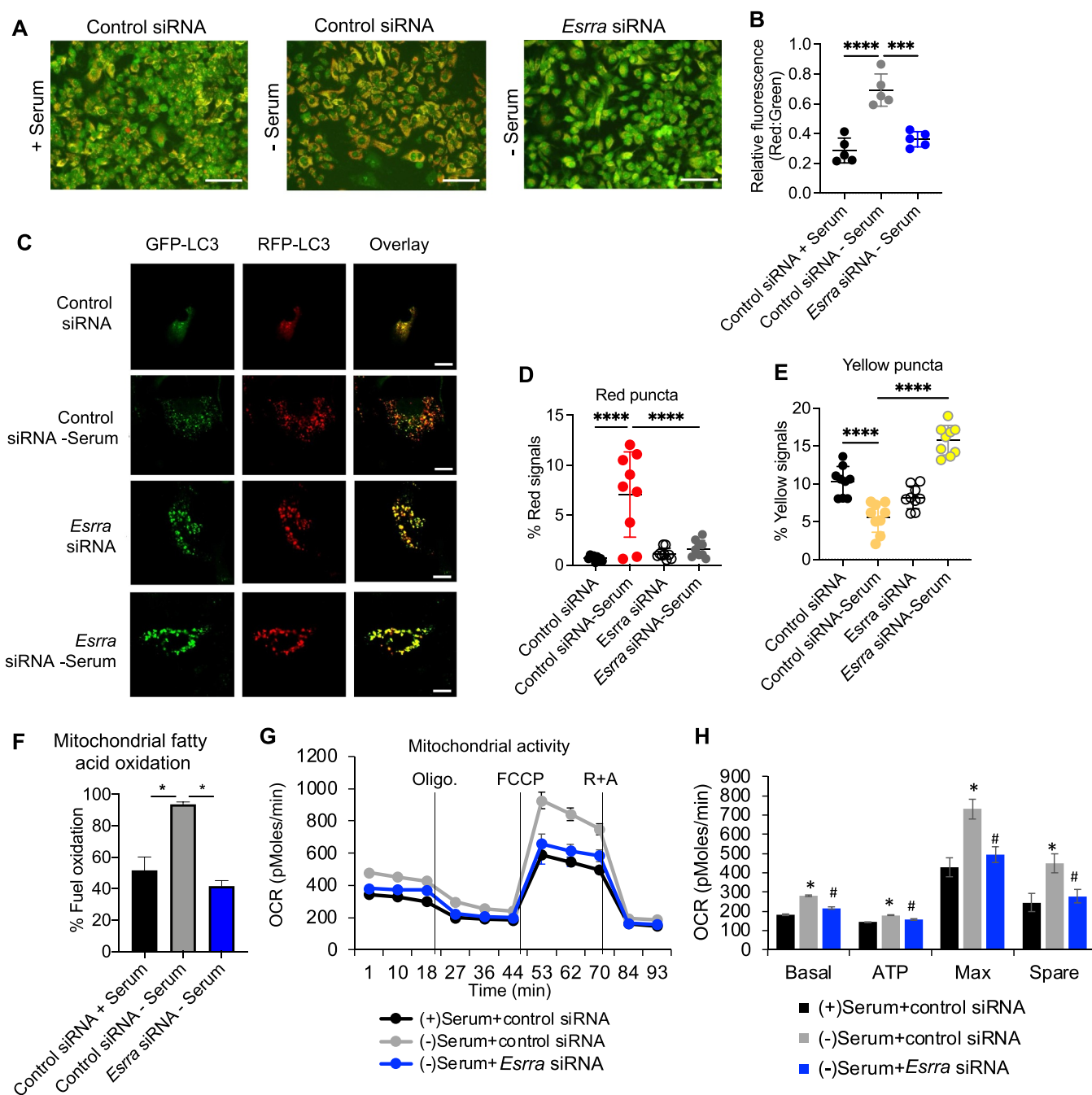


Figure 3. ESRRR regulated lysosome activity, autophagy flux and mitochondrial activity during serum starvation. (A) Microscopy image showing acridine orange staining of AML12 cells treated with control siRNA or si-*Esrra* with or without 24 h serum starvation. Images are representative of three fields per group and three independent experiments. Scale bars: 200 μ m. (B) Plot shows relative fluorescence that was measured using ImageJ (NIH, USA). $n = 5$ per group. (C) Microscopy image showing RFP-GFP-LC3 expression in AML12 cells treated with control siRNA or si-*Esrra* with or without 24-h serum starvation. Images are representative of three fields per group and three independent experiments. Scale bars: 5 μ m. (D and E) % red signals reflecting red puncta (D) for autolysosomes or % yellow signals reflecting yellow puncta (E) for autophagosomes. Colocalization analysis software CoLocalizer Pro 7.0.1 was used to analyze % red and yellow signals. (F) Mitochondrial fatty acid oxidation was analyzed in control siRNA and si-*Esrra* treated AML12 cells using Seahorse XFe96 analyzer. (G and H) Mitochondrial oxidative phosphorylation (OXPHOS) as oxygen consumption rate (OCR) was analyzed in control siRNA and si-*Esrra* treated AML12 cells using Seahorse XFe96 analyzer (G) and the parameters were calculated (H) as described in Methods section. Levels of significance: * $p < .05$; ** $p < .01$; *** $p < .001$; **** $p < .0001$.

S3E and F). Serum starvation significantly increased lysosome (L) and autolysosomal (AL) autophagic vesicles in AML12 cells, whereas, *Esrra* KD resulted in decreased autophagic vesicles with the accumulation of autophagosomes filled with undigested cargo. Moreover, we also used a lysosomal inhibitor, bafilomycin A₁, to demonstrate starvation-induced autophagy flux [13,34] as there was less accumulation of

MAP1LC3B-II in *Esrra* KD cells than control cells (Figures S3G and H), and more MAP1LC3B-II accumulation in *Esrra* overexpressed cells than control cells (Figure S3I and J).

ESRRR previously was shown to be a major regulator of mitochondrial biogenesis, β -oxidation of fatty acids, and mitophagy by inducing the expression of key genes involved in these processes [10,13]. In this connection, we found that

Esrra siRNA KD inhibited mitochondrial fatty acid fuel oxidation, respiratory activity, OXPHOS, and ATP production in AML12 cells undergoing starvation (Figure 3F-H). These findings demonstrated that ESRRA coordinately regulated autophagy and these key metabolic and energy production processes to enable an integrated response during starvation.

ESRRA regulation of ribosome-catalyzed translation of lysosome proteins in hepatic cells prevented cell death during prolonged starvation

We next examined ESRRA-RPLP1 regulation of lysosome and autophagy protein translation during prolonged starvation by puromycin-labeling proteins in cells grown in normal or serum free media either as basal or containing a highly specific ESRRA inverse agonist, C29 [15,30,35,36] (Figures S4A-C). C29 decreased ESRRA protein expression and prevented induction of RPLP1, reduced selective puromycin-labeling of proteins, and diminished LAMP2, CTSD, and MAP1LC3B-II protein expression. SQSTM1 significantly accumulated due to reduced lysosome activity and late-block autophagy. Furthermore, micrographs clearly showed that inhibition of ESRRA by C29 during 72-h serum starvation induced cell death (Figure S4D), suggesting that ESRRA regulation of adaptive protein translation was critical for cell survival during prolonged serum starvation. To determine whether the increased autophagy and lysosome protein expression at 72-h serum starvation was due to translational recovery or enhanced transcription of these genes, we performed RT-qPCR analysis in these samples, and found that although *Esrra*, *Rplp1*, *Lamp2*, *Ctsd*, *Map1lc3b*, and *Sqstm1* gene expression significantly increased at 72-h serum starvation, *Ctsd*, *Map1lc3b*, and *Sqstm1* gene expression increased even when ESRRA was inhibited by C29 (Figure S4E). Moreover, we also confirmed that inhibiting ESRRA using C29 during serum starvation in primary human hepatocytes decreased puromycin-labeling of proteins and induced significant cell death (Figure S4F and G). These findings were discordant with the protein expression data and demonstrated that the increased expression of lysosomal and autophagy proteins at 72-h serum starvation was primarily due to ESRRA-mediated RPLP1-dependent translation rather than increased transcription. The induction of *Ctsd*, *Map1lc3b*, and *Sqstm1* gene expression during prolonged starvation, even after C29 treatment, suggested there was alternative regulation by transcription factors such as TFEB and FOXOs rather than ESRRA [37,38]. Taken together, our data clearly showed that continuous replenishment of autophagy proteins was required to maintain autophagy flux and cell survival during prolonged starvation. Further, we confirmed that ESRRA regulation of autophagy flux included translation of lysosome proteins in addition to the transcriptional mechanisms described previously [10,29,39].

ESRRA, RPLP1, lysosome and autophagy proteins in mice were co-regulated during fasting and refeeding

To better understand ESRRA regulation of ribosome-dependent translation during starvation and its effects on lysosome-autophagy function *in vivo*, we analyzed liver tissues from mice fasted for 24 h and then refed mice for

6 h (Figure 4A,B). Consistent with our *in vitro* data, protein expression of ESRRA, RPLP1, LAMP2, CTSD, and MAP1LC3B-II increased significantly, whereas SQSTM1 expression significantly decreased during prolonged fasting suggesting there was activation of the ESRRA-RPLP1-lysosome pathway and increased autophagy flux during prolonged fasting. Interestingly, upon refeeding there was significantly reduced hepatic expression of ESRRA, RPLP1, LAMP2, CTSD, and MAP1LC3B-II expression whereas SQSTM1 was accumulated when compared to fed. These data strongly suggested reduced ESRRA/RPLP1-mediated adaptive translation led to decreased lysosomal activity and a late block in autophagy in refed mice [13,40].

To demonstrate that ESRRA/RPLP1-mediated adaptive translation was essential for autophagy *in vivo*, we examined the effects of inhibiting ESRRA in mice treated with the inverse agonist of ESRRA, XCT790 [13,41,42]. XCT790-treated mice had significantly decreased hepatic expression of ESRRA, RPLP1, LAMP2, CTSD, MAP1LC3B-II and increased SQSTM1 (Figures S5A and B). Electron micrographs also confirmed that hepatic lysosome/autolysosome number was significantly decreased in XCT790-treated mice compared to vehicle-treated controls, suggesting that ESRRA regulated lysosome synthesis (Figures S5C and D). Furthermore, we compared wild-type (WT) and *esrra* knockout (KO) mice in the fed state and after 24 h starvation (Figure 4C,D). In the fed state, *esrra* KO mice showed a significant decrease in RPLP1 expression and a downward trend in the expression of LAMP2 and MAP1LC3B-II proteins compared to WT mice. Fasting increased ESRRA, RPLP1, LAMP2, CTSD, and MAP1LC3B-II protein expression, and had no significant effect on SQSTM1 protein in WT mice. In *esrra* KO mice, these increases in the protein expression during starvation were significantly attenuated, and SQSTM1 expression increased during starvation suggesting that there was a late block in autophagy when ESRRA was not expressed (Figure 4C,D). Likewise, hepatic *esrra* overexpression in mice increased the hepatic expression of RPLP1, LAMP2, and CTSD proteins and promoted autophagy flux as evidenced by the increased MAP1LC3B-II and decreased SQSTM1 expression (Figure 4E,F).

To better understand ESRRA's effects on hepatic protein translation during starvation *in vivo*, we injected mice with vehicle (control) or C29 during starvation, and measured protein puromycin labeling at baseline, 8-, 24-, and 48-h starvation. Hepatic protein translation decreased from 8 to 24 h and then significantly increased at 48-h compared to 24 h in control mice suggesting there was some recovery at 48-h (Figure 5A,B). In contrast, there was a significant inhibition of overall puromycin labeling from 8 to 48 h starvation in C29-injected mice compared to their fed state (0 h). ESRRA, LAMP2, CTSD, and MAP1LC3B-II protein translation progressively increased from 8 h to 48 h starvation in vehicle-treated mice (Figure 5A,C-F). However, ESRRA, RPLP1, LAMP2, and CTSD protein translation was significantly lower in C29-treated mice than vehicle-treated mice at each time point. MAP1LC3B-II protein translation also was inhibited and SQSTM1 was increased in C29-treated mice starved for 24 h and 48 h (Figure 5A,C-F).

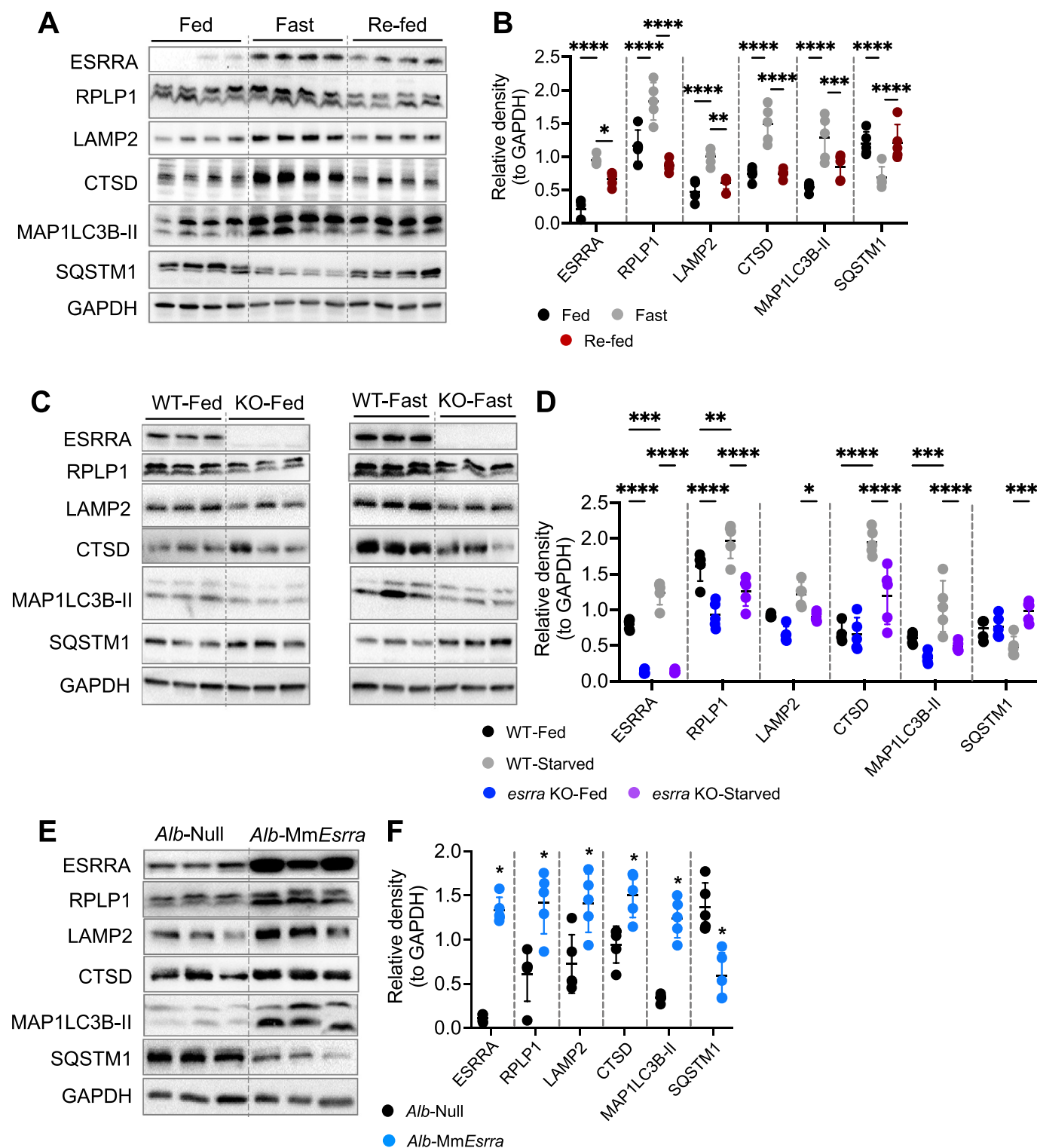


Figure 4. ESRRA regulated temporal changes in RPLP1-lysosome axis and autophagy in mice livers. (A) Representative western blots of fed, 24 h-fasted and 6 h-refed livers. (B) Plots represent relative density of corresponding western blots normalized to GAPDH ($n = 5$ per group). (C) Representative western blots of fed and 24 h starved livers from WT and *esrra* KO mice. (D) Plots represent relative density of corresponding western blots normalized to GAPDH ($n = 5$ per group). (E) Representative western blots of livers from liver-specific overexpressed *Esrra* (*Alb-MmEsrra*) or control (*Alb-null*) mice. (F) Plots represent relative density of corresponding western blots normalized to Gapdh ($n = 5$ per group). Levels of significance: * $p < .05$; ** $p < .01$; *** $p < .001$; **** $p < .0001$.

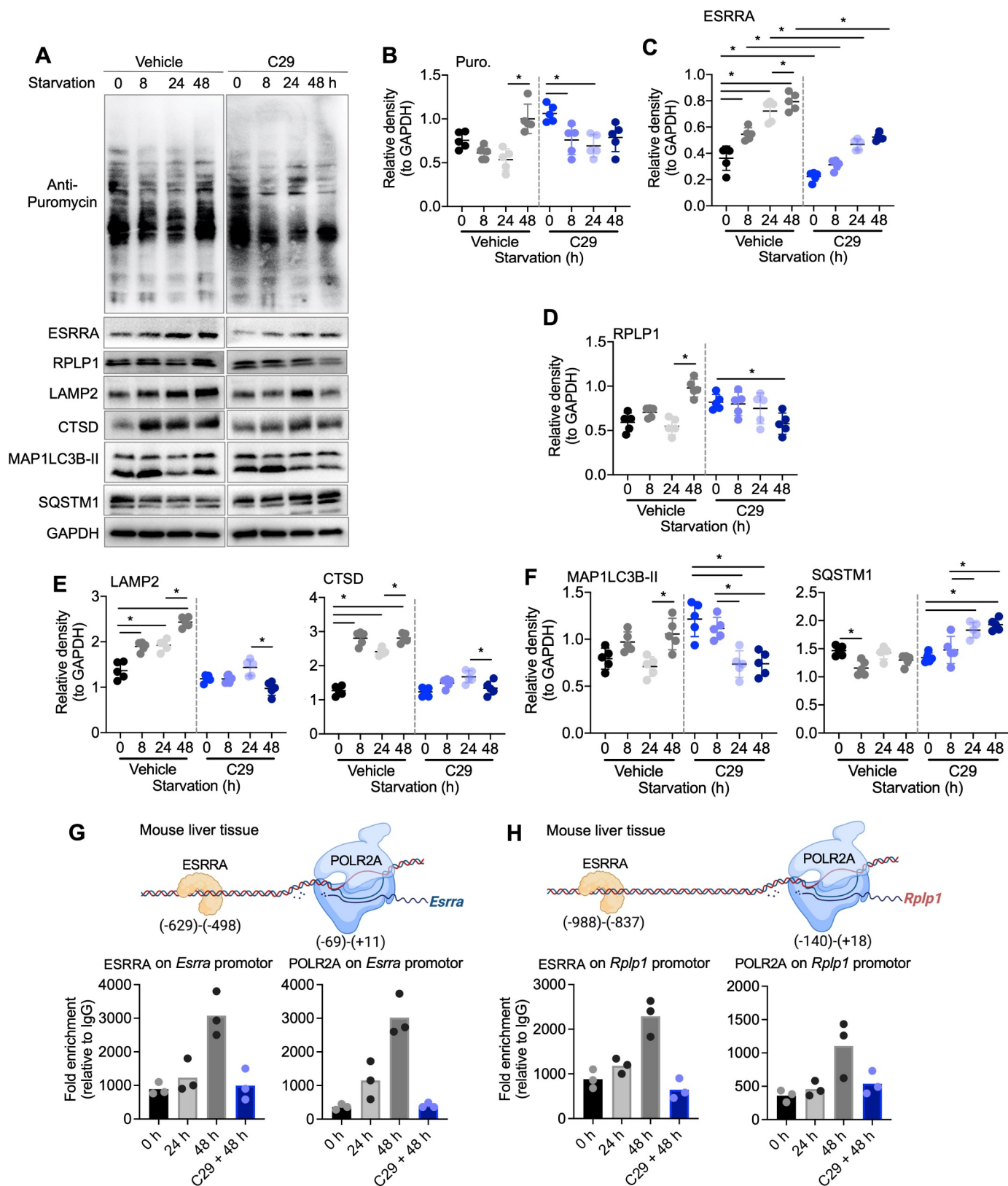


Figure 5. ESRRR regulated temporal changes in RPL1-lysosome axis and autophagy in mice livers. (A) Representative western blots of starved mice livers at indicated time points treated with vehicle or ESRRR inhibitor C29 (n = 5 per group). (B-F) Plots represent relative density of corresponding western blots normalized to GAPDH. (G and H) ChIP-qPCR analysis of ESRRR and POLR2A binding on *Esrra* or *Rplp1* promoters respectively. The experiment was performed three times independently. Levels of significance: *p < 0.05.

ESRRA and POLR2A binding to the ESRRA and RPLP1 promoters were necessary for autophagy-mediated β -oxidation of fatty acids

We identified strong ERREs binding sites on the *Esrra* and *Rplp1* promoters using previously published mouse liver ESRRA ChIP-seq databases [13,43] (Figure 2B). We then used chromatin immunoprecipitation-qPCR (ChIP-qPCR) assays to observe ESRRA and POLR2A binding on *Esrra* and *Rplp1* gene promoters at these ERREs and the TATA-box in the livers from mice starved for 24 h and 48 h treated with and without C29 (Figure 5G,H). Both ESRRA and POLR2A increased their binding to *Esrra* and *Rplp1* promoters in untreated mice at 48-h starvation while C29 completely inhibited ESRRA and POLR2A binding on *Esrra* and *Rplp1* gene promoters at this time point (Figure 5G,H). C29 treatment also significantly inhibited hepatic *Esrra* and *Rplp1* mRNA expression in mice starved for 48 h (Figure S5E). Interestingly, these mice nevertheless had higher *Lamp2*, *Ctsd*, *Map1lc3b* and *Sqstm1* mRNA expression than control mice, despite lower protein translation than controls suggesting alternative transcriptional mechanisms when ESRRA was inhibited (Figure S5E). Of note, ERR and ERs share homology and might influence each other's target gene, we observed that hepatic *Esrra* and its target genes' expression (*Acadm*, *Cpt1a*, *Pdk4* and *Got1*) were increased under 24 and 48 h starvation. Whereas ESRRA inhibition using C29 robustly inhibited starvation-induced expression of these genes (Figure S5F). Further, expression of *Esr1* and its target genes were not increased during starvation in male mice (Figure S5G). Since, the progressive increases in *Esrra* and *Rplp1* mRNAs correlated with increased protein translations and *Cpt1a* (key gene regulating mitochondrial fatty acid oxidation) expression during starvation in control mice, we observed serum β -hydroxybutyrate (β -HB; a marker of hepatic fatty acid β -oxidation regulated by lipophagy [13,44]) was significantly higher in control mice after 24 h starvation compared to 0 h, and further increased after 48 h starvation (Figure S5H). In contrast, β -HB did not further increase in C29-injected mice starved for 48 h. These data showed that ESRRA-dependent RPLP1-mediated translation of lysosome-autophagy proteins was required for sustained fatty acid β -oxidation during starvation *in vivo*.

Discussion

Our study provided significant insights into the mechanisms by which cells adapt to prolonged starvation, emphasizing the novel role of ESRRA in regulating adaptive protein translation. The findings highlighted the complex interplay between transcriptional and translational control orchestrated by ESRRA to maintain cellular homeostasis during nutrient deprivation (Figure S4I). Amino acid metabolism plays a critical role in adaptive translation during starvation where liver acts as the central hub for amino acid metabolism, ensuring a steady supply of amino acids for various metabolic processes and protein synthesis [45,46]. During prolonged starvation, the selective translation of lysosomal and autophagy-related proteins ensures the continuous recycling of amino

acids through autophagy, maintaining cellular homeostasis and supporting vital functions such as mitochondrial respiration and fatty acid oxidation [7,25]. While ESRRA's role in transcriptional regulation is well-established, its involvement in translation regulation represents a novel function. We demonstrated that ESRRA induces the expression of RPLP1, a ribosomal protein that enhances the translation of lysosomal and autophagy-related proteins. This selective translation is crucial for sustaining autophagy, a process that recycles cellular components to provide essential substrates during nutrient scarcity.

The mechanistic insights from our study align with the current understanding of the MTOR (mechanistic target of rapamycin kinase) pathway, a central regulator of cell growth and metabolism. MTOR activity is known to be inhibited during nutrient deprivation, leading to the suppression of general protein synthesis to conserve energy [47,48]. However, our data suggest that ESRRA can bypass this suppression by selectively promoting the translation of autophagy and lysosomal proteins via RPLP1. This selective translation is essential for maintaining cellular functions critical for survival during prolonged starvation. Interestingly, ESRRA's regulatory role may intersect with MTOR signaling. Previous study has shown that pharmacological MTOR inhibition led to ESRRA degradation [30]. Thus, the crosstalk between ESRRA and MTOR could represent a coordinated mechanism to balance protein synthesis and degradation, ensuring cellular homeostasis during metabolic stress. Future studies are warranted to explore this potential interaction in greater detail.

AMP-activated protein kinase (AMPK) is another key regulator of cellular energy homeostasis that is activated in response to low energy levels during fasting [49]. AMPK activation enhances catabolic pathways that generate ATP while inhibiting anabolic processes that consume ATP. Our findings suggest that ESRRA may work in concert with AMPK to regulate adaptive responses to nutrient deprivation. AMPK has been shown to phosphorylate and activate PPARGC1A, a coactivator of ESRRA, thereby enhancing ESRRA's transcriptional activity [10]. Furthermore, AMPK can directly inhibit MTOR signaling that may stabilize ESRRA to promoting autophagy [50]. This suggests a synergistic relationship between ESRRA and AMPK in promoting autophagy-lysosome function and maintaining energy balance. The interplay between these pathways highlights a complex regulatory network that ensures cells can efficiently respond to metabolic stress. Thus, the integration of ESRRA into existing metabolic pathways highlights its versatile role in cellular metabolism. By coordinating with MTOR and AMPK signaling, ESRRA may ensure a balanced response to nutrient deprivation, promoting lysosome-autophagy function and maintain energy homeostasis. This multifaceted regulatory role highlighted the importance of ESRRA in metabolic adaptation and its potential as a therapeutic target.

In summary, our study elucidates a novel function of ESRRA in regulating adaptive protein translation during prolonged starvation. The ESRRA-RPLP1 pathway selectively enhances the translation of autophagy and lysosomal proteins, ensuring cellular survival under nutrient-scarce

conditions. The interplay between ESRRA, MTOR, and AMPK signaling pathways highlights a complex regulatory network that maintains metabolic homeostasis. These findings provide a deeper understanding of ESRRA's role in metabolism and highlight its potential as a therapeutic target for metabolic diseases. Future research should further explore the regulatory mechanisms and therapeutic applications of ESRRA in metabolic health. It is possible that agents increasing ESRRA expression or mimicking its activity potentially may enhance ESRRA-RPLP1-lysosome protein translation. Such compounds, by functioning as "fasting" analogs, could be useful therapeutically to increase hepatic fatty acid β -oxidation in metabolic disorders such as MASH. It is however noteworthy that the induction of ESRRA and the inhibition of MTOR activity also may have synergistic effects during fasting in MASH [12,30]. Interestingly, ESRRA enhanced autophagy in other cell types [10,13,27–29,51] so this pathway may be involved in tissues other than the liver. Currently, the role(s) of ESRRA-RPLP1-lysosome protein translation on autophagy in other hepatic, metabolic, or malignant conditions is not known. It remains to be determined whether the decreased ESRRA expression observed in metabolic diseases such as MASH, obesity, and diabetes cause aberrant starvation response, autophagy, or protein translation that could be restored by induction of the ESRRA-RPLP1-lysosome protein translation pathway.

Materials and methods

Animal studies

Fed-Fast-Refed mice

8–10-weeks-old male C57BL/6J mice ($n = 5/\text{group}$) were fed with normal chow control diet (NCD) and starved overnight before starting the experiment for synchronization. After one day, mice were kept in new empty cages (without husk bedding and NCD) for 24 (Fast group), and few mice from Fast group were refed for 6 h with NCD (Refed). Mice that had not undergone fasting or refeeding after synchronization were considered as the Fed group.

Starvation studies

8–10 weeks old male C57BL/6J mice ($n = 5/\text{group}$) were fed with normal chow control diet (NCD) and starved overnight before starting the experiment for synchronization. After one day, mice were kept in new empty cages (without husk bedding) for 8, 24, 48 h. C29 (10 mg/kg body weight; kindly provided by Prof. Donald McDonnell, Duke University School of Medicine, USA) was started injecting *i.p.* from the synchronization day to 48 h fasting day for the chronic inhibition of ESRRA [30]. Cycloheximide (Chx; 10 mg/kg body weight; Sigma-Aldrich, C7698) was injected *i.p.* 60 min before euthanization for translation inhibition, while puromycin (Puro, 20 mg/kg body weight; Sigma-Aldrich, P7255) was injected *i.p.* 30 min before euthanization for puromycin labeling of proteins to understand rate of translation.

Esrra KO mice

Esrra KO mice are described elsewhere [30,52]. *Esrra* WT and *Esrra* KO mice ($n = 5/\text{group}$) were synchronized by overnight fasting and starved for 24 h after two days or left fed. Later, mice were euthanized, blood and liver tissues were collected for mRNA and protein analysis.

Alb-MEsrra overexpression

For liver-specific expression, we used AAV8-mediated gene delivery of the *MEsrra* gene cloned under the control of the mouse *Alb* promoter (Vector Biolabs, AAV-258720). 8-weeks-old male C57BL/6J mice ($n = 5/\text{group}$) were used for liver-specific *esrra* overexpression (*Alb-MEsrra*). Mice were generated by injecting AAV8-*Alb-MEsrra* (5×10^{11} gc/mice) via tail vein and housed for four weeks with no other intervention [53]. We injected AAV8-*Alb-Null* which does not contain any DNA sequence under the transcriptional control of the *Alb* promoter as controls. Later, mice were euthanized, blood and liver tissues were collected for mRNA and protein analysis.

General mouse care and ethics statement

Mice were purchased from InVivos, Singapore and, housed in hanging polycarbonate cages under a 12 h/12 h light/dark schedule at Duke-NUS vivarium. Mice were simple randomized before grouping and fed different diets and normal water, or fructose treated *ad libitum*. Animals were euthanized in CO₂ chambers. All mice were maintained according to the Guide for the Care and Use of Laboratory Animals (NIH publication no. One.0.0. Revised 2011), and the experiments performed were approved by the IACUCs at SingHealth (2015/SHS/1104) and (2020/SHS/1549).

Serum triglycerides and β -hydroxybutyrate (β -HB/Ketone bodies) measurements

Serum triglycerides (TG), and β -HB was measured using Triglyceride Colorimetric Assay Kit (Cayman 10,010,303) and β -HB (Ketone Body) Colorimetric Assay Kit (Cayman 700,190).

Cell cultures

AML12 cells. (ATCC®, CRL-2254™) were cultured as indicated elsewhere [54,55]. Starvation medium (DMEM:F12 mix with Pen/Strep lacking serum, ITS [Gibco 41,400,045] and dexamethasone [Sigma-Aldrich, D2915]) was used for serum-starvation experiments. To analyze the rate of translation, puromycin (10 $\mu\text{g}/\text{ml}$) was added for 15 min before harvest [18] whereas C29 (5 μM) was added to media for indicated time to inhibit ESRRA [30]. Bafilomycin A₁ (5 nM; Sigma-Aldrich, B1793) was used to analyze autophagy flux [13].

Primary human hepatocytes. (ScienCell, 5200) were cultured as indicated elsewhere [53,56]. Puromycin (10 $\mu\text{g}/\text{ml}$) was added for 15 min before harvest [18] whereas C29 (5 μM) was added to media for the indicated time [30].

Gene manipulation in cultured cells

Gene knockdown in vitro. Silencer Select siRNAs (Thermo Fisher Scientific, s4829, s4830, and s4831) or ON-

TARGETplus Smartpool siRNAs (Horizon Discoveries, L-040772-00-0010) against *Esrra*, and Silencer Select siRNA (Thermo Fisher Scientific, s234520) for *Rplp1* gene knock-down were used in AML12 cells. Negative siRNA (Silencer Negative Control No. 1 siRNA; Thermo Fisher Scientific, AM4611) was used as a negative control. Transfections were carried out in AML12 cells in a 12-well or 6-well plate or four-well chambered slides or 24-well Seahorse XF plate using 30 nM of the above indicated siRNAs and negative control siRNA with Lipofectamine™ RNAiMAX (Thermo Fisher Scientific 13,778,150) following the reverse transfection protocol, as indicated elsewhere [13,54].

Gene overexpression in vitro. ORF sequence of *Esrra* (Gene ID: 26379) and *Rplp1* (Gene ID: 56040) genes were cloned in a pcDNA3.1(+)-C-6His plasmid by Genescript Limited (Hong Kong) to get *Esrra*_OMu13026C_pcDNA3.1(+)-C-6His and *Rplp1*_OMu11118C_pcDNA3.1(+)-C-6His constructs for *Esrra* and *Rplp1* overexpression in AML12 cells, respectively. Transfections were carried out in a 12-well plate or 6-well plate using Lipofectamine 3000 (Thermo Fisher Scientific, L3000015) following the reverse transfection protocol, as described elsewhere [13]. Empty pcDNA3.1(+)-C-6His vector was used as control.

RNA isolation and RT-qPCR analysis of gene expression

RNA isolation and RT-qPCR for measuring gene expression were performed as described previously [13]. Predesigned KiCqStart SYBR Green optimized primers from Sigma-Aldrich (KSPQ12012) were used for RT-qPCR.

Protein isolation and western blotting analysis of protein expression

Protein isolation and western blotting analysis of protein expression were performed as described previously [13]. Primary antibodies for puromycin (1:25,000 dilution; Merck, MABE343), 1:1000 dilution of *ESRR*A (Abcam, ab16363; Millipore, 07-662; and Cell Signaling Technology [CST], 13826S), *RPLP1* (Invitrogen, PA5-103540), *LAMP2* (Invitrogen, PA1-655), *CTSD* (Santa Cruz Biotechnology, sc377299), *GAPDH* (CST, 2118), *MAP1LC3B-II/LC3B* (CST, a2775), and *SQSTM1/p62* (CST, 5114) were used. Horseradish peroxidase-conjugated secondary antibodies recognizing mouse (Santa Cruz Biotechnology, sc2954) and rabbit (Santa Cruz Biotechnology, sc2955) immunoglobulin Gs (IgGs) were used. Blots were observed on Image Lab software (Bio-Rad) and densitometric analysis was performed using ImageJ software (NIH, Bethesda, MD, USA) normalized to *GAPDH* as loading controls.

Immunoprecipitation of puromycin-incorporated proteins

Protein immunoprecipitation was performed using Dynabeads™ Protein G for Immunoprecipitation (Thermo Fisher Scientific, 10007D) as per manufacturer's protocol. Non-denaturing lysis buffer (as described at Abcam) was used to prepare tissue homogenate. Puromycin (1:5,000 dilution; Merck, MABE343), or 4 µg normal rabbit IgG as control (Sigma-Aldrich, 12-370) was used for affinity-isolation assay.

Western blot analysis for the detection of pulled down proteins was performed as described above.

Label-free quantitative proteomic analysis

Label-free quantitative analysis of proteins, recovered from pooled triplicates each group, by LC-MS/MS was performed by NonovogeneAIT (Singapore) as described below.

Protein quality test. BSA standard protein solution was prepared according to the instructions of Bradford protein quantitative kit (Bio-Rad 5,000,201), with gradient concentration ranged from 0 to 0.5 g/L. BSA standard protein solutions and sample solutions with different dilution multiples were added into a 96-well plate to fill up the volume to 20 µL, respectively. Each gradient was repeated three times. To the plate was added 180 µL G250 dye solution quickly and placed at room temperature for 5 min, after which the absorbance at 595 nm was detected. The standard curve was drawn with the absorbance of standard protein solution and the protein concentration of the sample was calculated. Twenty µg of the protein sample was loaded for 12% SDS-PAGE gel electrophoresis, wherein the concentrated gel was performed at 80 V for 20 min, and the separation gel was performed at 120 V for 90 min. The gel was stained by Coomassie Brilliant Blue R-250 and decolorized until the bands were visualized clearly.

Trypsin treatment. An aliquot (120 µg) of each protein sample was taken and the volume was made up to 100 µL with dissolution buffer, 1.5 µg trypsin (Sigma-Aldrich, T8658) and 500 µL of 100 mM TEAB buffer (Merck 18,597) were added, sample was mixed and digested at 37°C for 4 h. And then, 1.5 µg trypsin and CaCl₂ were added, sample was digested overnight. Formic acid was mixed with digested sample, adjusted pH under 3, and centrifuged at 12,000 g for 5 min at room temperature. The supernatant was slowly loaded to the C18 desalting column (Thermo Fisher Scientific 89,852), washed with washing buffer (0.1% formic acid, 3% acetonitrile) 3 times, then eluted by some elution buffer (0.1% formic acid, 70% acetonitrile). The eluents of each sample were combined and lyophilized.

LC-MS/MS analysis. Mobile phase A (100% water, 0.1% formic acid) and B solution (80% acetonitrile, 0.1% formic acid) were prepared. The lyophilized powder was dissolved in 10 µL of solution A, centrifuged at 14,000 g for 20 min at 4°C, and 1 µg of the supernatant was injected into a home-made C18 Nano-Trap column (2 cm × 75 µm, 3 µm). Peptides were separated in a home-made analytical column (15 cm × 150 µm, 1.9 µm), using a linear gradient elution. The separated peptides were analyzed by Q Exactive HF-X mass spectrometer (Thermo Fisher), with ion source of Nanospray Flex™ (ESI, spray voltage of 2.3 kV and ion transport capillary temperature of 320°C. Full scan range from m/z 350 to 1500 with resolution of 60,000 (at m/z 200), an automatic gain control (AGC) target value was 3 × 10⁶ and a maximum ion injection time was 20 ms. The top 40 precursors of the highest abundant in the full scan were selected and fragmented by higher energy collisional dissociation (HCD) and analyzed in MS/MS, where resolution was

15,000 (at m/z 200), the automatic gain control (AGC) target value was 1×10^5 , the maximum ion injection time was 45 ms, a normalized collision energy was set as 27%, an intensity threshold was 2.2×10^4 , and the dynamic exclusion parameter was 20 s. The raw data of MS detection was named as “.raw”.

The identification and quantification of protein. All resulting spectra were searched against Mus_musculus_uniprot_2019.01.18.fasta (85165 sequences) database by the search engines: Proteome Discoverer 2.2 (Thermo Fisher Scientific, PD 2.2). The search parameters are set as follows: mass tolerance for precursor ion was 10 ppm and mass tolerance for product ion was 0.02 Da. Carbamidomethyl was specified as fixed modifications, Oxidation of methionine (M) was specified as dynamic modification, and acetylation was specified as N-Terminal modification in PD 2.2. A maximum of 2 missed cleavage sites were allowed. In order to improve the quality of analysis results, the software PD 2.2 further filtered the retrieval results: Peptide Spectrum Matches (PSMs) with a credibility of more than 99% was identified PSMs. The identified protein contains at least 1 unique peptide. The identified PSMs and protein were retained and performed with FDR no more than 1.0%. The protein quantitation results were statistically analyzed by T-test. The proteins whose quantitation significantly different between experimental and control groups, ($p < 0.05$ and $|\log_2FC| \geq 2$ (ratio ≥ 4 or ratio ≤ 0.25 [fold change, FC])), were defined as differentially expressed proteins (DEP).

The functional analysis of protein and DEP. Gene Ontology (GO) and KEGG (Kyoto Encyclopedia of Genes and Genomes) were used to analyze the protein family and pathway whereas Targeting Protein-Protein Interactions (PPIs) for protein-protein interactions on EnrichR platform (the Ma'ayan Lab, NY, USA) [57–59].

Fluorescence imaging of the cells

Autophagy flux analysis. ptfLC3 (Addgene 21,074; deposited by Prof. Tamotsu Yoshimori [60]) was transfected using Lipofectamine 3000 reagent (Thermo Fisher Scientific, L3000015) in *Esrra* knockdown or control cells as described in the manufacturer's protocol. After 48 h of transfection, cells were serum starved for further 24 h. The cells were then fixed with 4% paraformaldehyde for 15 min and washed three times with $1 \times$ PBS (Merck, P7059). Slides were washed and wet mounted in VECTASHIELD Antifade Mounting Medium (Vector Laboratories, H-1000-10). Fluorescence imaging was performed using LSM710 Carl Zeiss (Carl Zeiss Microscopy GmbH, Oberkochen, Germany) confocal microscope at $40 \times$ magnification.

Acridine orange (AO) staining. Cells were transfected and grown in 24-well plate for 48 h and serum starved for a further 24 h. Thereafter, cells were incubated with $1 \mu\text{g/ml}$ of AO (Sigma-Aldrich, A9231) in PBS for 30 min at 37°C , and observed under a fluorescence microscope as described elsewhere [61].

Transmission electron microscopy (TEM) imaging of the liver tissues

Fresh liver tissue was placed in fixative (2% paraformaldehyde and 3% glutaraldehyde in cacodylate buffer, pH 7.4) and stored at 4°C . TEM analysis was performed as described previously [13]. Images were taken using the Olympus EM208S transmission electron microscope (Japan) at $\times 10,000$ magnifications. Mean number of lysosomes per TEM field from untreated control and XCT790-treated mouse liver samples was calculated from a total of 10 random fields per treatment.

Mitochondrial oxygen consumption rate (OCR) measurement by Seahorse extracellular flux analyzer

Seahorse extracellular flux analyzer XFe96 (Agilent) was used for mitostress test, and mitochondrial fatty acid fuel oxidation analysis. Seahorse Wave Desktop software was used for report generation and data analysis while GraphPad PRISM 9 was used for statistical analysis and data presentation. 10000 AML12 cells were seeded on XFe-96-well culture microplates and the assays were performed as described previously [62].

Chromatin Immunoprecipitation (ChIP)-qPCR in AML12 cells and ChIPseq in liver tissues

ChIP-qPCR was performed as described previously [13,63]. For *Esrra* binding on the *Esrra* gene, primer pairs [ATGCATGGTCCCAGAGTCAG (forward) and CTGGTTTGC GAGTTCCTCAA (reverse)] were used to amplify – 629 to – 498 region on *Esrra* promoters in AML12 cells. For POLR2A binding, a primer pair [ATTAGCATAGGGCACCTGGC (forward) and CGACCACCGTGGCTGAC (reverse)] was used to amplify – 69 to + 11 region in AML12 cells. However, on the *Rplp1* gene promoter, for *Esrra* binding, primer pairs [AGCTTCTTTGTG GTCCTGAGATT (forward) and ACCCCTCAGGTTAGGGTA CA (reverse)] were used to amplify – 988 to – 837 region on the *Rplp1* promoter in AML12 cells. For POLR2A binding on *Rplp1* gene promoter, a primer pair [CAATCGCACCGGAAGTCGAA (forward) and GACCAGTCCACCTATATACGCC (reverse)] were used to amplify – 140 to + 18 region in AML12 cells.

ChIPseq methodology is provided elsewhere [30].

Polysome profiling in vitro using sucrose gradients

AML12 cells were cultured with BSA (0.5% as control; Merck, A9418), PA (0.5 mm for 24 h; Merck, P0500) or PA with si-*Esrra*, washed with cold PBS and subsequently lysed on ice using a lysis buffer containing Tris-Cl (pH 7.4, 20 mM), NaCl (150 mM), MgCl_2 (5 mM), NP40 (1%; Merck, NP40), DTT (1 μM), cycloheximide (100 $\mu\text{g/ml}$), and cOmplete™ EDTA-free Protease Inhibitor (1X; Merck 11,873,580,001). The lysate was then homogenized by passing through a 27 G needle five times. Cellular debris was separated by centrifuging at $20,000 \times g$ for 10 min at 4°C . Following this, the lysate was loaded onto a 10–50% sucrose (Merck 84,097) gradient, which had been previously prepared with the Gradient Master (Science Services, B108–2). Polysome profiling was subsequently conducted, and fractions were collected using the Biocomp fractionator, in tandem with TRIAX. The data was plotted using GraphPad PRISM software.

Statistical analysis

Individual culture experiments were performed in triplicate and repeated at least three times independently using matched controls; the data were pooled ($n = 3/\text{group}$), and statistical analysis was performed. Animal studies were performed as per the approved IACUC protocol, and the statistical analysis were performed ($n = 4\text{--}5/\text{group}$) as per the biostatistician's advice. Results are expressed as mean \pm SD for all in vitro and in vivo experiments. Normality of the data was analyzed by Shapiro-Wilk test, then a parametric analysis was performed using unpaired student's t-test, one-way ANOVA or two-way ANOVA followed by Tukey's multiple-comparisons test, wherever applicable. The statistical significance of differences was assessed as $*p < 0.05$; $**p < 0.01$; $***p < 0.001$; $****p < 0.0001$. All statistical tests were performed using Prism 9 for Mac OS X (GraphPad Software).

Acknowledgements

The authors like to acknowledge that the research is funded by the Ministry of Health (MOH), and National Medical Research Council (NMRC), Singapore, grant number NMRC/OFYIRG/0002/2016 and MOH-000319 (MOH-OFYIRG19may-0002), Duke/Duke-NUS Research Collaboration Pilot Project Award (Duke/Duke-NUS/RECA(Pilot)/2022/0060), and KBrFA (Duke-NUS-KBrFA/2023/0075) to BKS; NMRC/OFYIRG/077/2018 to MT; and CSAI19may-0002 to PMY; Duke-NUS Medical School and Estate of Tan Sri Khoo Teck Puat Khoo Pilot Award (Collaborative) Duke-NUS-KP(Coll)/2018/0007A to JZ.

Disclosure statement

No potential conflict of interest was reported by the author(s).

Funding

This work is also partially supported by grants from the Louisiana Clinical and Translational Science Center [NIGMS 2U54GM104940], the National Heart Lung and Blood Institute, NIH, USA [NHLBI R01HL146462-01], and the Khoo Bridge Fund, Singapore [KBrFA/2022/0060] to SG. The illustrations were made on BioRender.com.

Data availability statement

The data will be available on request.

ORCID

Brijesh K. Singh  <http://orcid.org/0000-0003-4615-3988>

References

- [1] Akiyama Y, Ivanov P. Oxidative stress, transfer RNA metabolism, and protein synthesis. *Antioxid Redox Signal*. 2023;40(10--12):715–735. doi: 10.1089/ars.2022.0206
- [2] Liu B, Qian SB. Translational reprogramming in cellular stress response. *Wiley Interdiscip Rev RNA*. 2014;5(3):301–315. doi: 10.1002/wrna.1212
- [3] Spriggs KA, Bushell M, Willis AE. Translational regulation of gene expression during conditions of cell stress. *Mol Cell*. 2010;40(2):228–237. doi: 10.1016/j.molcel.2010.09.028
- [4] Jaud M, Philippe C, Di Bella D, et al. Translational regulations in response to endoplasmic reticulum stress in cancers. *Cells*. 2020;9(3):540. doi: 10.3390/cells9030540
- [5] Yin Z, Liu X, Ariosa A, et al. Psp2, a novel regulator of autophagy that promotes autophagy-related protein translation. *Cell Res*. 2019;29(12):994–1008. doi: 10.1038/s41422-019-0246-4
- [6] Feng L, Chen Y, Xu K, et al. Cholesterol-induced leucine aminopeptidase 3 (LAP3) upregulation inhibits cell autophagy in pathogenesis of NAFLD. *Aging (Albany NY)*. 2022;14(7):3259–3275. doi: 10.18632/aging.204011
- [7] Yamamuro T, Nakamura S, Yanagawa K, et al. Loss of RUBCN/rubicon in adipocytes mediates the upregulation of autophagy to promote the fasting response. *Autophagy*. 2022;18(11):1–11. doi: 10.1080/15548627.2022.2047341
- [8] Sinha RA, Singh BK, Yen PM. Reciprocal crosstalk between autophagic and endocrine signaling in metabolic homeostasis. *Endocr Rev*. 2017;38(1):69–102. doi: 10.1210/er.2016-1103
- [9] Allaire M, Rautou PE, Codogno P, et al. Autophagy in liver diseases: time for translation? *J Hepatol*. 2019;70(5):985–998. doi: 10.1016/j.jhep.2019.01.026
- [10] Tripathi M, Yen PM, Singh BK. Estrogen-related receptor alpha: an under-appreciated potential target for the treatment of metabolic diseases. *Int J Mol Sci*. 2020;21(5):21. doi: 10.3390/ijms21051645
- [11] Park HS, Song JW, Park JH, et al. TXNIP/VDUP1 attenuates steatohepatitis via autophagy and fatty acid oxidation. *Autophagy*. 2020;17(9):1–16. doi: 10.1080/15548627.2020.1834711
- [12] B'Chir W, Dufour CR, Ouellet C, et al. Divergent role of estrogen-related receptor α in lipid- and fasting-induced hepatic steatosis in mice. *Endocrinology*. 2018;159(5):2153–2164. doi: 10.1210/en.2018-00115
- [13] Singh BK, Sinha RA, Tripathi M, et al. Thyroid hormone receptor and ERR α coordinately regulate mitochondrial fission, mitophagy, biogenesis, and function. *Sci Signal*. 2018;11(536):11. doi: 10.1126/scisignal.aam5855
- [14] Laganier J, Tremblay GB, Dufour CR, et al. A polymorphic autoregulatory hormone response element in the human estrogen-related receptor α (erra) promoter dictates peroxisome proliferator-activated receptor γ coactivator-1 α control of erra expression. *J Biol Chem*. 2004;279(18):18504–18510. doi: 10.1074/jbc.M313543200
- [15] Perry MC, Dufour CR, Tam IS, et al. Estrogen-related receptor- α coordinates transcriptional programs essential for exercise tolerance and muscle fitness. *Mol Endocrinol*. 2014;28(12):2060–2071. doi: 10.1210/me.2014-1281
- [16] Audet-Walsh E, Giguere V. The multiple universes of estrogen-related receptor α and γ in metabolic control and related diseases. *Acta Pharmacol Sin*. 2015;36(1):51–61. doi: 10.1038/aps.2014.121
- [17] Xia H, Dufour CR, Giguere V. ERR α as a bridge between transcription and function: role in liver metabolism and disease. *Front Endocrinol (Lausanne)*. 2019;10:206. doi: 10.3389/fendo.2019.00206
- [18] Aviner R. The science of puromycin: from studies of ribosome function to applications in biotechnology. *Comput Struct Biotechnol J*. 2020;18:1074–1083. doi: 10.1016/j.csbj.2020.04.014
- [19] Goodman CA, Hornberger TA. Measuring protein synthesis with SUNSET: a valid alternative to traditional techniques? *Exerc Sport Sci Rev*. 2013;41(2):107–115. doi: 10.1097/JES.0b013e3182798a95
- [20] Ravi V, Jain A, Ahamed F, et al. Systematic evaluation of the adaptability of the non-radioactive SUNSET assay to measure cardiac protein synthesis. *Sci Rep*. 2018;8(1):4587. doi: 10.1038/s41598-018-22903-8
- [21] Schmidt EK, Clavarino G, Ceppi M, et al. SUNSET, a nonradioactive method to monitor protein synthesis. *Nat Methods*. 2009;6(4):275–277. doi: 10.1038/nmeth.1314
- [22] Perucho L, Artero-Castro A, Guerrero S, et al. y LLeonart ME, Cajal S, Li ME, Bernier G. RPLP1, a crucial ribosomal protein for embryonic development of the nervous system. *PLOS ONE*. 2014;9(6):e99956. doi: 10.1371/journal.pone.0099956
- [23] Feng Y, He D, Yao Z, et al. The machinery of macroautophagy. *Cell Res*. 2014;24(1):24–41. doi: 10.1038/cr.2013.168

- [24] Manning BD. Adaptation to starvation: translating a matter of life or death. *Cancer Cell*. 2013;23(6):713–715. doi: [10.1016/j.ccr.2013.05.012](https://doi.org/10.1016/j.ccr.2013.05.012)
- [25] Zhou J, Singh BK, Ho JP, et al. MED1 mediator subunit is a key regulator of hepatic autophagy and lipid metabolism. *Autophagy*. 2021;17(12):1–19. doi: [10.1080/15548627.2021.1899691](https://doi.org/10.1080/15548627.2021.1899691)
- [26] Salazar G, Cullen A, Huang J, et al. SQSTM1/p62 and PPARGC1A/PGC-1alpha at the interface of autophagy and vascular senescence. *Autophagy*. 2020;16(6):1092–1110. doi: [10.1080/15548627.2019.1659612](https://doi.org/10.1080/15548627.2019.1659612)
- [27] Casaburi I, Avena P, De Luca A, et al. Estrogen related receptor α (ERR α) a promising target for the therapy of adrenocortical carcinoma (ACC). *Oncotarget*. 2015;6(28):25135–25148. doi: [10.18632/oncotarget.4722](https://doi.org/10.18632/oncotarget.4722)
- [28] Kim S, Lee AJ, Yeo MK, et al. Clinicopathological profiling of LC3B, an autophagy marker, and ESRRA (Estrogen-related Receptor-alpha) in muscle-invasive bladder cancer. *Anticancer Res*. 2018;38:2429–2437.
- [29] Kim SY, Yang CS, Lee HM, et al. ESRRA (estrogen-related receptor α) is a key coordinator of transcriptional and post-translational activation of autophagy to promote innate host defense. *Autophagy*. 2018;14(1):152–168. doi: [10.1080/15548627.2017.1339001](https://doi.org/10.1080/15548627.2017.1339001)
- [30] Chaveroux C, Eichner LJ, Dufour CR, et al. Molecular and Genetic Crosstalks between mTOR and ERR α are key determinants of rapamycin-induced nonalcoholic fatty liver. *Cell Metab*. 2013;17(4):586–598. doi: [10.1016/j.cmet.2013.03.003](https://doi.org/10.1016/j.cmet.2013.03.003)
- [31] Kolapalli SP, Nielsen TM, Frankel LB. Post-transcriptional dynamics and RNA homeostasis in autophagy and cancer. *Cell Death Differ*. 2023;32(1):27–36. doi: [10.1038/s41418-023-01201-5](https://doi.org/10.1038/s41418-023-01201-5)
- [32] Tan HWS, Anjum B, Shen HM, et al. Lysosomal inhibition attenuates peroxisomal gene transcription via suppression of PPARGC1A and PPARGC1A levels. *Autophagy*. 2019;15(8):1455–1459. doi: [10.1080/15548627.2019.1609847](https://doi.org/10.1080/15548627.2019.1609847)
- [33] Eriksson I, Vainikka L, Persson HL, et al. Real-time monitoring of lysosomal membrane permeabilization using acridine orange. *Methods Protoc*. 2023;6(4):6. doi: [10.3390/mps6040072](https://doi.org/10.3390/mps6040072)
- [34] Klionsky DJ, Abdel-Aziz AK, Abdelfatah S, et al. Guidelines for the use and interpretation of assays for monitoring autophagy (4th edition) 1. *Autophagy*. 2021;17(1):1–382. doi: [10.1080/15548627.2020.1797280](https://doi.org/10.1080/15548627.2020.1797280)
- [35] Park S, Chang CY, Safi R, et al. ERR α -regulated lactate metabolism contributes to resistance to targeted therapies in breast cancer. *Cell Rep*. 2016;15(2):323–335. doi: [10.1016/j.celrep.2016.03.026](https://doi.org/10.1016/j.celrep.2016.03.026)
- [36] Patch RJ, Searle LL, Kim AJ, et al. Identification of diaryl ether-based ligands for estrogen-related receptor α as potential antidiabetic agents. *J Med Chem*. 2011;54(3):788–808. doi: [10.1021/jm101063h](https://doi.org/10.1021/jm101063h)
- [37] Di Malta C, Cinque L, Settembre C. Transcriptional regulation of autophagy: mechanisms and diseases. *Front Cell Dev Biol*. 2019;7:114. doi: [10.3389/fcell.2019.00114](https://doi.org/10.3389/fcell.2019.00114)
- [38] Palmieri M, Impey S, Kang H, et al. Characterization of the CLEAR network reveals an integrated control of cellular clearance pathways. *Hum Mol Genet*. 2011;20(19):3852–3866. doi: [10.1093/hmg/ddr306](https://doi.org/10.1093/hmg/ddr306)
- [39] Kim S, Lee JY, Shin SG, et al. ESRRA (estrogen related receptor alpha) is a critical regulator of intestinal homeostasis through activation of autophagic flux via gut microbiota. *Autophagy*. 2021;17(10):2856–2875. doi: [10.1080/15548627.2020.1847460](https://doi.org/10.1080/15548627.2020.1847460)
- [40] Tripathi M, Singh BK, Zhou J, et al. Vitamin B(12) and folate decrease inflammation and fibrosis in NASH by preventing syntaxin 17 homocysteinylation. *J Hepatol*. 2022;77(5):1246–1255. doi: [10.1016/j.jhep.2022.06.033](https://doi.org/10.1016/j.jhep.2022.06.033)
- [41] Lynch C, Zhao J, Huang R, et al. Identification of estrogen-related receptor α agonists in the Tox21 compound library. *Endocrinology*. 2018;159(2):744–753. doi: [10.1210/en.2017-00658](https://doi.org/10.1210/en.2017-00658)
- [42] Teng CT, Hsieh JH, Zhao J, et al. Development of novel cell lines for high-throughput screening to detect estrogen-related receptor alpha modulators. *SLAS Discov*. 2017;22(6):720–731. doi: [10.1177/2472555216689772](https://doi.org/10.1177/2472555216689772)
- [43] Dufour CR, Levasseur MP, Pham NH, et al. Genomic convergence among ERR α , PROX1, and BMAL1 in the control of metabolic clock outputs. *PLOS Genet*. 2011;7(6):e1002143. doi: [10.1371/journal.pgen.1002143](https://doi.org/10.1371/journal.pgen.1002143)
- [44] Sinha RA, Farah BL, Singh BK, et al. Caffeine stimulates hepatic lipid metabolism by the autophagy-lysosomal pathway in mice. *Hepatology*. 2014;59(4):1366–1380. doi: [10.1002/hep.26667](https://doi.org/10.1002/hep.26667)
- [45] Gretzmeier C, Eiselein S, Johnson GR, et al. Degradation of protein translation machinery by amino acid starvation-induced macroautophagy. *Autophagy*. 2017;13(6):1064–1075. doi: [10.1080/15548627.2016.1274485](https://doi.org/10.1080/15548627.2016.1274485)
- [46] Pain VM. Translational control during amino acid starvation. *Biochimie*. 1994;76(8):718–728. doi: [10.1016/0300-9084\(94\)90076-0](https://doi.org/10.1016/0300-9084(94)90076-0)
- [47] Fonseca BD, Smith EM, Yelle N, et al. The ever-evolving role of mTOR in translation. *Semin Cell Dev Biol*. 2014;36:102–112. doi: [10.1016/j.semcdb.2014.09.014](https://doi.org/10.1016/j.semcdb.2014.09.014)
- [48] Morita M, Gravel SP, Chenard V, et al. mTORC1 controls mitochondrial activity and biogenesis through 4E-BP-dependent translational regulation. *Cell Metab*. 2013;18(5):698–711. doi: [10.1016/j.cmet.2013.10.001](https://doi.org/10.1016/j.cmet.2013.10.001)
- [49] Townsend LK, Steinberg GR. AMPK and the endocrine control of metabolism. *Endocr Rev*. 2023;44(5):910–933. doi: [10.1210/endrev/bnad012](https://doi.org/10.1210/endrev/bnad012)
- [50] Gwinn DMS, Shaw RJ. AMPK control of mTOR signaling and growth. In: Tamanoi F, editor. *The Enzyme*. Academic Press; 2010. p. 49–75.
- [51] Suresh SN, Chavalmame AK, Pillai M, et al. Modulation of autophagy by a small molecule inverse agonist of ERR α is neuroprotective. *Front Mol Neurosci*. 2018;11:109. doi: [10.3389/fnmol.2018.00109](https://doi.org/10.3389/fnmol.2018.00109)
- [52] Sailland J, Tribollet V, Forcet C, et al. Estrogen-related receptor α decreases RHOA stability to induce orientated cell migration. *Proc Natl Acad Sci USA*. 2014;111(42):15108–15113. doi: [10.1073/pnas.1402094111](https://doi.org/10.1073/pnas.1402094111)
- [53] Dong J, Viswanathan S, Adami E, et al. Hepatocyte-specific IL11 cis-signaling drives lipotoxicity and underlies the transition from NAFLD to NASH. *Nat Commun*. 2021;12(1):66. doi: [10.1038/s41467-020-20303-z](https://doi.org/10.1038/s41467-020-20303-z)
- [54] Bruinstroop E, Zhou J, Tripathi M, et al. Early induction of hepatic diiodinase type 1 inhibits hepatosteatosis during NAFLD progression. *Mol Metab*. 2021;53:101266. doi: [10.1016/j.molmet.2021.101266](https://doi.org/10.1016/j.molmet.2021.101266)
- [55] Tripathi M, Yen PM, Singh BK. Protocol to generate senescent cells from the mouse hepatic cell line AML12 to study hepatic aging. *STAR Protoc*. 2020 July 1;1(2):100064. doi: [10.1016/j.xpro.2020.100064](https://doi.org/10.1016/j.xpro.2020.100064)
- [56] Widjaja AA, Dong J, Adami E, et al. Redefining IL11 as a regeneration-limiting hepatotoxin and therapeutic target in acetaminophen-induced liver injury. *Sci Transl Med*. 2021;13(597). doi: [10.1126/scitranslmed.aba8146](https://doi.org/10.1126/scitranslmed.aba8146)
- [57] Chen EY, Tan CM, Kou Y, et al. Enrichr: interactive and collaborative HTML5 gene list enrichment analysis tool. *BMC Bioinformatics*. 2013;14(1):128. doi: [10.1186/1471-2105-14-128](https://doi.org/10.1186/1471-2105-14-128)
- [58] Kuleshov MV, Jones MR, Rouillard AD, et al. Enrichr: a comprehensive gene set enrichment analysis web server 2016 update. *Nucleic Acids Res*. 2016;44(W1):W90–7. doi: [10.1093/nar/gkw377](https://doi.org/10.1093/nar/gkw377)
- [59] Xie Z, Bailey A, Kuleshov MV, et al. Gene set knowledge discovery with enrichr. *Curr Protoc*. 2021;1(3):e90. doi: [10.1002/cpz1.90](https://doi.org/10.1002/cpz1.90)
- [60] Kimura N, Kumamoto T, Kawamura Y, et al. Expression of autophagy-associated genes in skeletal muscle: an experimental model of chloroquine-induced myopathy. *Pathobiology*. 2007;74(3):169–176. doi: [10.1159/000103376](https://doi.org/10.1159/000103376)
- [61] Tripathi M, Zhang CW, Singh BK, et al. Hyperhomocysteinemia causes ER stress and impaired autophagy that is reversed by vitamin B supplementation. *Cell Death Dis*. 2016;7(12):e2513. doi: [10.1038/cddis.2016.374](https://doi.org/10.1038/cddis.2016.374)
- [62] Singh BK, Tripathi M, Sandireddy R, et al. Decreased autophagy and fuel switching occur in a senescent hepatic cell model system. *Aging (Albany NY)*. 2020;12(14):13958–13978. doi: [10.18632/aging.103740](https://doi.org/10.18632/aging.103740)
- [63] Singh BK, Sinha RA, Zhou J, et al. FoxO1 deacetylation regulates thyroid hormone-induced transcription of key hepatic gluconeogenic genes. *J Biol Chem*. 2013;288(42):30365–30372. doi: [10.1074/jbc.M113.504845](https://doi.org/10.1074/jbc.M113.504845)